Biochimica et Biophysica Acta, 681 (1982) 152–160
Elsevier Biomedical Press

BBA 41106

EFFECT OF NEIGHBORING CHARGES AND EXTERNAL FIELDS ON PHOTOSYNTHETIC ELECTRON TRANSFER

S. RACKOVSKY and H. SCHER

Xerox Corporation, 800 Phillips Road-114, Webster, NY 14580 (U.S.A.)

(Received September 14th, 1981)
(Revised manuscript received March 2nd, 1982)

Key words: Electron transfer; Photosynthesis; Reaction center; Electric field effect; Tunneling matrix element

We investigate the influence of neighboring charges and external electric fields on the rate of an electron-transfer step in bacterial photosynthesis. It is shown that reaction center geometry plays a crucial role in determining the dynamics of photosynthetic electron transfer, by modulating not only the tunneling matrix element, but also, through the coulombic interaction, the Franck-Condon factor. An estimate is made of the intersite energy difference under operative conditions, and the relationship between this quantity and reaction center geometry is discussed. The photosynthetic reduction of the primary reaction center quinone in the presence of reduced secondary quinone is studied. Constraints are placed on the location of the secondary quinone in the reaction center, and the temperature dependence of the transfer rate is predicted. Finally, the effect of externally applied electric fields is studied, and it is shown that this leads to a method for testing the hypothesis that the transfer of an electron from bacteriopheophytin to ubiquinone is an activationless process.

Introduction

The study of bacterial photosynthesis offers an excellent opportunity to assess quantitatively the relationship between structure and function in an important biological system. In recent years, several picosecond spectroscopic measurements [1–8] have been performed on isolated bacterial reaction centers. These studies have cast considerable light on the sequence of electron-transfer steps which are the primary physical events in the overall photosynthetic reaction. These primary events can be summarized in three steps:

$$(BChl)_2BPhQ_IQ_{II} \xrightarrow{h\nu} (BChl)_2^*BPhQ_IQ_{II} \quad (1)$$

$$(BChl)_2^*BPhQ_IQ_{II} \xrightarrow{\tau_1} (BChl)_2^+BPh^-Q_IQ_{II} \quad (2)$$

$$(BChl)_2^+BPh^-Q_IQ_{II} \xrightarrow{\tau_2} (BChl)_2^+BPhQ_I^-Q_{II} \quad (3)$$

Here $(BChl)_2$ is a bacteriochlorophyll dimer, BPh a molecule of bacteriopheophytin, and Q_I and Q_{II} are, respectively, 'primary' and 'secondary' molecules of ubiquinone-10.

It has been shown [1–8] that the lifetime, τ_1, of the excited dimer created in step 1 is 10 ps or less; that the lifetime of the BPh^- radical anion, τ_2, is approx. 150 ps; and that the rate of step 3 is nearly temperature independent, down to 200 K.

The rate measurements are able to give some information about distances between the various electron sites, when taken together with ap-

Abbreviations: BChl, bacteriochlorophyll, BPh, bacteriopheophytin.

0005-2728/82/0000–0000/$02.75

propriate theoretical models. Information about the orientations of the various reaction center components as well as additional distance data, has been obtained by ESR measurements [9]. Thus, fairly detailed estimates of reaction center structure have been built up. These have been summarized by Dutton et al. [9].

Two principal theoretical models of the photosynthetic electron-transfer process have been advanced, those of Jortner [10] and of Redi and Hopfield [11]. The rate of electron transfer can be written as a product of two terms – the square of a tunneling matrix element and a Franck-Condon factor. Jortner [10] assumes a conventional exponential behavior for the tunneling matrix element as a function of intersite distance, and uses a multiphonon theory of the Franck-Condon factors operating in the photosynthetic reaction center. By using the experimentally measured rates and assuming values for various parameters which enter into the theory, an estimate of the tunneling matrix element can be derived, from which the distance between sites follows using the postulated exponential form. Redi and Hopfield [11] develop a more detailed theory of the tunneling matrix element, which takes into account its energy dependence. Despite their rather different approaches to the tunneling matrix element, and the different values of the various model parameters used, both approaches predict very similar distances between the various reaction center sites. These are summarized in Table I, together with the experimental estimates.

In order to distinguish between the various models and further refine them more experimental parameters are needed. One aspect of the photosynthetic electron-transfer problem which has received no theoretical attention, and which we shall investigate in this work, is the influence of electric fields on the electron-transfer rates. These fields can be of two types – coulombic fields arising from the presence of a neighboring charge, as in step 3, or externally applied electric fields, as used in voltage-clamping experiments [12]. As an example of the type of question raised by the coulombic interaction, one may consider the proper choice of the energy difference between the two sites in step 3. Attempts to measure this quantity experimentally have rested on electrochemical determination of the midpoint voltages of the BPh/BPh^- and Q/Q^- couples. As pointed out by Dutton et al. [9], these are equilibrium measurements, and therefore there is some question as to whether the values obtained apply on the very rapid time scale and in the very different molecular environment characteristic of step 3. It should also be noted, however, that the presence of $(BChl)_2^+$ in the immediate neighborhood of the two sites makes an additional, geometry-dependent contribution to the redox energy. We shall show below that this can be very large, and discuss the relationship between redox energy and geometry.

Another experimentally observable consequence of the coulombic interaction is the decrease in the rate of step 3 when the secondary quinone is reduced. This electron-transfer process, which has been observed by Pellin et al. [13], can be written:

$$(BChl)_2^+ BPh^- Q_I Q_{II}^- \xrightarrow{\tau_{2'}} (BChl)_2^+ BPh Q_I^- Q_{II}^- \qquad (3')$$

We shall discuss below the constraints placed on reaction center geometry by the observed rate decrease.

We shall also investigate the effect of externally applied electric fields on the rate of step 3. It will be seen that this effect is dependent on the relative orientation of the reaction center and electric field, and that it provides a method for testing proposed models of reaction center energetics.

In Section II we discuss the calculational approach we shall adopt in these investigations.

TABLE I

ESTIMATED AND MEASURED DISTANCES (Å) WITHIN THE PHOTOSYNTHETIC REACTION CENTER

	Reference		
	10	11	23
$R((BChl)_2-BPh)$	9.2	9 ± 1.5	10
$R(BPh-Q_I)$	10.1	10	10
$R((BChl)_2-Q_I)$	19.1	22	≥ 15

II. Methods

We shall calculate electron-transfer rates using an expression derived, with the chemical-rate formalism of Holstein [14,15], by Scher and Holstein [16]. This formalism, which yields results in excellent numerical agreement with the multiphonon approach, has the advantage of providing a particularly simple form for the electron-transfer rate – simple enough, in fact, to be evaluated on a hand calculator. At the same time dependences on various model parameters are of a relatively simple functional form.

Before recalling the relevant formula, we establish the model potentials with which we shall work. We denote by V_i the vibrational potential at site i when the electron is located at i. Then we have:

$$V_1 = (\hbar\omega/2)(q+\lambda)^2 + \Delta/2 \tag{4a}$$

$$V_2 = (\hbar\omega/2)(q-\lambda)^2 - \Delta/2 \tag{4b}$$

where q and λ are dimensionless configuration coordinates defined in Ref. 16, $\hbar\omega$ is the vibrational quantum of the active vibrational mode, and Δ the energy difference between the two sites. The derivation of these formulae from the standard multiphonon Hamiltonian is straightforward, and is given by Scher and Holstein [14–16]. With this notation, the rate of electron transfer is given [16] by:

$$\nu_{\pm} = (2\pi J^2/\hbar^2\omega)\left[4\pi\gamma(\delta^2 + \operatorname{cosech}^2\xi)^{1/2}\right]^{-1/2} \times \exp[\pm(\Delta/2k_BT) - F] \tag{5}$$

where

$$F = 2\gamma\left[\coth\xi - (\delta^2 + \cosh^2\xi)^{1/2} + \delta\sinh^{-1}(\delta\sinh\xi)\right] \tag{6}$$

and

$$\delta = \Delta/4E_a \tag{7}$$

$$\gamma = 2E_a/\hbar\omega \tag{8}$$

$$E_a = \hbar\omega\lambda^2/2 \tag{9}$$

$$\xi = \hbar\omega/2k_BT \tag{10}$$

The positive and negative signs in Eqn. 5 refer to the forward ($1 \rightarrow 2$) and reverse ($2 \rightarrow 1$) electron-transfer rates, respectively. It will also be convenient to define a dimensionless electron-transfer rate by:

$$\bar{\nu}_{\pm} = \nu_{\pm}/(2\pi J^2/\hbar^2\omega) \tag{11}$$

which is just the Franck-Condon factor.

Both Redi and Hopfield [11] and Jortner [10] account for the temperature independence of τ_2 by assuming that step 3 is an 'activationless' process – i.e., that V_2 intersects V_1 at $q = -\lambda$, so that there is no barrier to electron transfer from site 1 (BPh) to site 2 (Q_I). (Note that this is equivalent to the condition $\delta = 1$ in Eqns. 5 and 6.) This assumption places constraints on the values of the parameters which can be chosen. In view of the fact that the chemical rate approach is more akin to the multiphonon approach of Jortner, particularly in its treatment of the tunneling matrix element, our discussion will center on the parameter set chosen by Jortner. These values are $\Delta = 2400\ \text{cm}^{-1}$, $\hbar\omega = 400\ \text{cm}^{-1}$, $\lambda = 1.75$, $J = 4\ \text{cm}^{-1}$.

As pointed out by Scher and Holstein [14–16], the effect of external charges and fields can be included in Eqns. 5 and 6 (or indeed in any electron-transfer formalism) in a straightforward and physically reasonable approximation through their effect on Δ. Thus, in the presence of N external charges $\{Z_i\}$ located at $\{r_i\}$, and an external field E, Δ can be written:

$$\Delta = \Delta_0 + \sum_{i=1}^{N} (ZZ_i/\epsilon)(R_{1i}^{-1} - R_{2i}^{-1}) + ZE\cdot r_{12} \tag{12}$$

Here

$$\Delta_0 = \varepsilon_1 - \varepsilon_2 \tag{13}$$

is the value of Δ in the absence of external charges and fields, but under operational conditions as discussed in Section I:

$$r_{12} = r_1 - r_2 \tag{14}$$

$$R_{ij} = |r_i - r_j| \tag{15}$$

Z is the charge of the particle being transferred, and ϵ the dielectric constant. Eqns. 5, 6 and 12 will provide the tools for the discussion which follows.

III. Relationship between Δ_0 and geometry

In this section we shall demonstrate that the use of a postulated reaction center geometry and the measured electron-transfer rate for step 3 can lead to an estimate of Δ_0 under operative conditions. We shall discuss the relationship between reaction center geometry and Δ_0, and the limits this relationship places on Δ_0 and other model parameters.

As we remarked above, our discussion will center on the parameter set used by Jortner [10] in his discussion of step 3. It happens that the use of these parameters to calculate ν_+ gives precisely the rate observed for step 3 by Pellin et al. [13] in the absence of Q_{II}^-. This must be regarded as fortuitous in view of the various uncertainties present in both experiment and theory; nevertheless, it suggests that this parameter set provides a reasonable basis for discussion. In what follows we therefore take $\Delta = 2400\ \text{cm}^{-1}$.

If we then take values of $R_{13} = 9.2$ Å and $R_{23} = 19.1$ Å (Table I and Fig. 1), we arrive at a value of Δ_0 from the equation:

$$\Delta = \Delta_0 - (e^2/\epsilon_1)(1/R_{13} - 1/R_{23}) \tag{16}$$

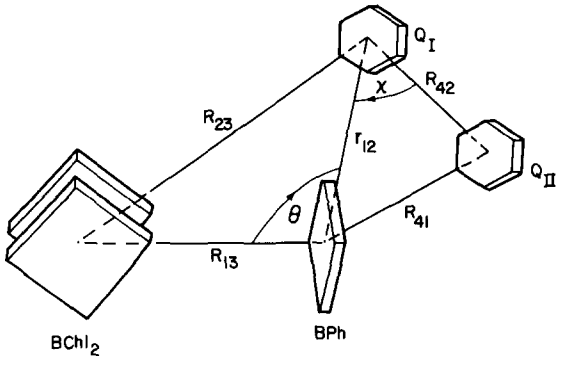

Fig. 1. Schematic illustration of reaction center geometry, showing notation for distances and angles. (From Tiede, D.M. and Dutton, P.L., personal communication.)

TABLE II

OPERATIVE VALUES OF Δ_0 USING THE GEOMETRY OF JORTNER [10]

ϵ	Δ_0 (eV)
1	1.11
2	0.71
3	0.57
4	0.50
5	0.46

The resulting values of Δ_0 are shown in Table II. The reduction in the operative value of Δ due to the coulombic interaction ranges from 35 to 73%. Clearly, the coulombic interaction has a profound influence on the operative value of Δ, and hence on the electron-transfer rate. For example, using Eqns. 5 and 6 and $\epsilon_1 = 3$, it can be shown that the neighboring charge causes an increase in electron-transfer rate of more than 6-fold. (The same calculation using the parameters of Redi and Hopfield [11] at $\epsilon_1 = 3$ gives a reduction in Δ of 39%.) This influence is in addition to that of factors such as solvent environment and time scale, which also cause Δ to differ from the value determined by equilibrium electrochemical measurements.

The foregoing considerations emphasize the primary importance of the reaction center geometry in determining the energetics, and hence the kinetics, of the electron-transfer process. This ability to alter physical processes through appropriate location of charges is one of the general connections between structure and function in biological systems. It has been suggested [17,18], for example, that in the visual process, the correct positioning of an external charge in the neighborhood of the retinal moiety is responsible for tuning the absorption spectrum of the rhodopsin molecule to various wavelengths.

In view of the great importance of reaction center geometry, it is of interest to ask what variation in reaction center geometry is necessary to accomodate variations in Δ_0. For example, a frequently encountered estimate of Δ_0 is approx. 0.5 eV (Kaufmann, K.J., Parson, W.W. and Dutton, P.L., personal communications). As can be seen from Table II, this value of Δ_0 results from the

geometry of Jortner [10] if $\epsilon_1 = 4$. One may also ask what geometry is required to produce $\Delta_0 = 0.5$ eV when $\epsilon_1 = 3$ (a typical value used in other biological systems [19]). Eqn. 16 can be rearranged to give:

$$1/R_{23} = \epsilon_1(\Delta - \Delta_0)/e^2 + 1/R_{13} \tag{17}$$

Another constraint is imposed by the condition:

$$\boldsymbol{R}_{23} + \boldsymbol{r}_{12} = \boldsymbol{R}_{13} \tag{18}$$

where all vectors are presumed to connect molecule centers. Since the $(BChl)_2$–BPh and BPh–Q_I distances (R_{13} and r_{12}, respectively) determined experimentally are in close agreement with theoretical estimates (Table I), we will take these distances as fixed at the values of Jorner [10], and focus on the $(BChl)_2$–Q_I distance (R_{23}), or, alternatively, on the angle θ between $\boldsymbol{r}_{12}$ and $\boldsymbol{R}_{13}$. When $\theta = 180°$ the reaction center geometry is linear and:

$$|\boldsymbol{R}_{23}| = |\boldsymbol{R}_{13}| + |\boldsymbol{r}_{12}| \tag{19}$$

Use of Eqns. 17 and 18 with $\Delta = 2400$ cm^{-1} shows that a value of $R_{23} = 15.0$ Å, corresponding to $\theta = 101.5°$, is necessary to give $\Delta_0 = 0.5$ eV with $\epsilon_1 = 3$. Inasmuch as this value of R_{23} is probably too low to correspond to experiment, one may speculate that the local dielectric constant is larger than expected, perhaps due to the presence of polarized π-electron systems; or, indeed, that $\Delta_0 \approx 0.5$ eV is a low estimate. In Fig. 2, we show R_{23} and θ vs. Δ_0 for $\epsilon_1 = 3$ and 4. It will be seen that as Δ_0 varies from 0.5 to 0.572 eV (a variation of 14.4%), R_{23} ($\epsilon_1 = 3$) varies from 15.0 to 19.3 Å (a 29% variation) and the geometry goes from almost right-angular to linear. Thus, improved experimental definition of R_{23} and a reasonable estimate of ϵ_1 should make it possible to put fairly narrow limits on Δ_0.

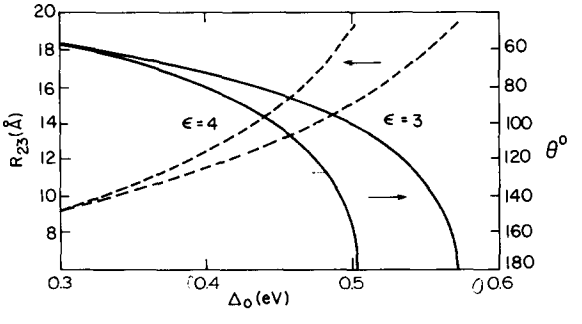

Fig. 2. R_{23} and θ plotted vs. Δ_0 for $\epsilon = 3$ and 4 (from Eqns. 17 and 18).

We may also note that, if a rate could be determined for the process:

$$(BChl)_2BPh^- Q_I Q_{II} \xrightarrow{\tau_{2''}} (BChl)_2BPhQ_I^- Q_{II} \tag{3''}$$

in which $(BChl)_2^+$ is reduced before electron transfer, use of Eqns. 5 and 6 would permit a numerical determination of Δ_0.

IV. Location of Q_{II}

The same considerations can be used to place limits on the position of Q_{II} in the reaction center. Pellin et al. [13] have measured the rate of electron-transfer reaction, step 3′, and shown that the reduction of Q_{II} causes a decrease in the rate of electron transfer from BPh to Q_I. From the measured rate of step 3′, we will derive a relationship between the BPh–Q_{II} and Q_I–Q_{II} distances.

Using Eqns. 5 and 6, with the same values of $\hbar\omega$, λ, and J used in Section III, it can be shown numerically that the value of Δ corresponding to the observed rate of electron transfer in the presence of Q_{II}^- is $\Delta = 1150$ cm^{-1} ($= 0.14$ eV). The equation for Δ' (where the prime distinguishes Δ' from Δ, the value in the absence of Q_{II}^-) is:

$$\Delta' = \Delta + (e^2/\epsilon_2)(1/R_{41} - 1/R_{42}) \tag{21}$$

where $R_{41} = R(Q_{II}$–BPh) and $R_{42} = R(Q_{II}$–$Q_I)$. Note that the sign of the correction term in Eqn. 18 is opposite to that in Eqn. 16, reflecting the fact that the external charge is now negative. Note also that ϵ_2, the effective local dielectric constant, need not be equal to ϵ_1 (Eqn. 16).

As before, we have the additional constraint (Fig. 1):

$$\boldsymbol{R}_{41} + \boldsymbol{r}_{12} = \boldsymbol{R}_{42} \tag{22}$$

Taking $\Delta = 2400$ cm^{-1} enables us to determine R_{42} and χ as functions of r_{12} and ϵ_2. From these

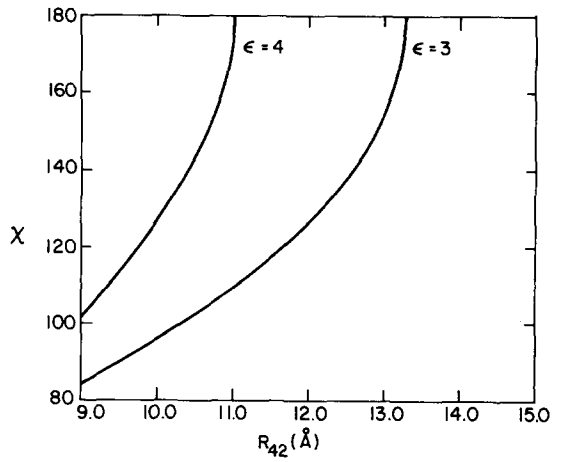

Fig. 3. χ plotted vs. R_{42} for $\epsilon = 3$ and 4 (from Eqns. 21 and 22).

results R_{41} can also be determined, using Eqn. 22. In Fig. 3 results are presented for R_{24} with $\epsilon_2 = 3$ and 4, with r_{12} fixed as before at 10.13 Å.

It can be seen that the rough estimate of Q_{II} location made by Pellin et al. [13] is ruled out by our calculation. With $\epsilon_2 = 3$, R_{42} can be no more than 13.3 Å, a distance which corresponds to a colinear geometry. The arrangement proposed in Ref. 6, i.e. colinear with $R_{24} \approx 17$ Å, is possible only if $\epsilon_2 = 2$. In fact, an independent experimental determination of the location of Q_{II} in the reaction center would lead to an estimate of the local dielectric constant ϵ_2.

We can also predict the temperature dependence of process 3′. This is shown, together with that of process 3, in Fig. 4. It can be seen that process 3 is predicted to exhibit a rate which increases slightly as temperature decreases from 300 K ($\hbar\omega/2k_BT) = 0.96$); this is in keeping with experiment [10]. On the other hand, the rate of process 3′ is predicted to show essentially no temperature dependence over the entire range of experimentally attainable temperatures. This experiment, which has not yet been performed, would constitute a dramatic demonstration of the effect of neighboring charges on an electron-transfer rate.

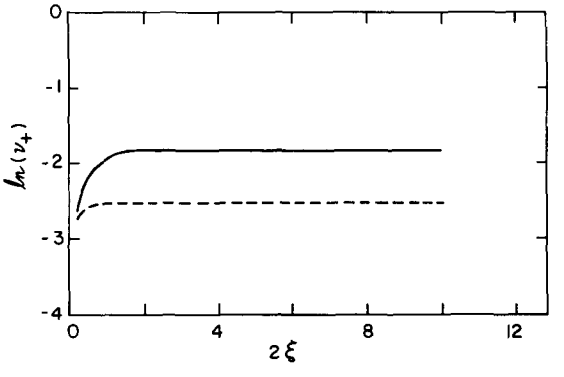

Fig. 4. Temperature variation of the reduced rate of electron transfer between BPh and Q_I, with (— — —) and without (———) Q_{II} reduced.

V. External electric fields and electron transfer

Externally applied electric fields have been used in several ways to study photosynthetic systems. For example, voltage clamping has been used [12] to show that reaction centers can be reconstituted in an artificial membrane in such a way as to preserve their directional electron-transfer properties. Experiments have also been performed on the electric-field-induced biochemistry of plant photosynthetic systems [20]. In this section we will show how the coupling between reaction center orientation and electric field can be used to investigate the assumption that step 3 is activationless. This assumption has been made because of the temperature independence of τ_2. It is conceivable, though, that step 3 is an activated process, with parameters such that the transition from activated to activationless behavior occurs above room temperature.

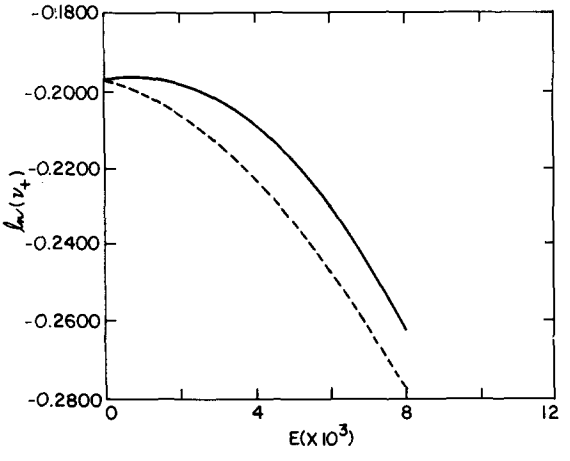

Fig. 5. Plot of ln ν_+ vs. field strength for $\phi = 45°$ (———) and 135° (— — —); $\delta = 1$, $T = 300$ K. The field strength E is in statv./cm.

It would therefore be of interest to examine this point experimentally.

From Eqn. 12, the effect of an electric field on Δ can be written

$$\Delta' = \Delta - eEr_{12}\cos\phi, \tag{23}$$

where Δ is the value in the absence of a field, and ϕ the angle between r_{12} and E. If the electron-transfer process is activationless, the rate can be expected to be maximal when the second term in Eqn. 23 is equal to zero. (Actually, the chemical rate theory predicts that the maximum in ν_+ should occur at a value of δ which is slightly less than unity at finite temperatures. It can be shown * that this difference is experimentally negligible.) This can be accomplished in two ways – by setting either $\phi = 90°$ or $E = 0$. This suggests two experimental approaches – measuring ν_+ either as a function of reaction center orientation at fixed field strength, or at fixed orientation as a function of field strength. We present calculated data for the latter approach, which is probably experimentally more feasible.

Figs. 5–7 show results at $\phi = 45$ and 135°, as a function of field strength. When $\delta = 1$, $\ln \nu_+$ decreases with E at all angles $\phi \neq 90°$. When $\delta \neq 1$, the rate is essentially constant for angles on one side of 90°, and decreases for angles on the other side of 90°. This suggests that measurement of the electron-transfer rate at a single orientation of reaction centers, as a function of E, for two opposite orientations of E, is sufficient to determine whether the process is activated or activationless. This type of measurement could be performed, for example, on a sample of reaction centers oriented in an artificial membrane. The main experimental difficulty is the high value of the field strength necessary for measurable change in the transfer rate.

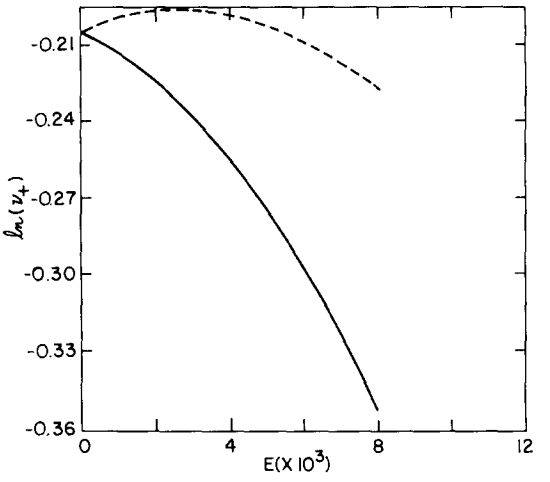

Fig. 6. Same as Fig. 5, $\delta = 0.75$.

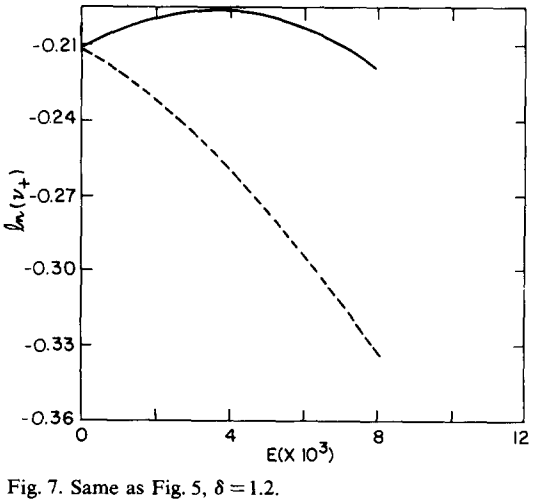

Fig. 7. Same as Fig. 5, $\delta = 1.2$.

* Using Eqns. 5, 6 and 11, it is straightforward to derive an equation for the value of δ at the maximum of ν_+. Differentiating Eqn. 5 gives:

$$(2k_BT)^{-1} - (\hbar\omega)^{-1}\sinh^{-1}(\delta\sinh\xi) - \delta\left(8E_a\left(\delta^2 + \mathrm{cosech}^2\xi\right)\right)^{-1} = 0$$

Writing:

$$\delta = 1 + \Omega$$

and linearizing the first equation in Ω leads to the solution:

$$\Omega = -\tanh^2\xi\left[(8E_a/\hbar\omega)e^{-\xi}\left(\sinh\xi + \cosh\xi\tanh^2\xi\right) + \tanh^2\xi\left(1 - 2\tanh^2\xi\right)\right]^{-1}$$

At $T = 300$ K, with the parameters used throughout the paper, $\Omega = -0.061$, so that $\delta_{max} = 0.939$. At low values of $|E|$, the variation in $\ln \nu_+$ is quite small, so that deviations of ϕ_{max} from 90° (or equivalently, of δ_{max} from 1) are probably not detectable. At $|E| = 0.4 \cdot 10^4$ statvolt/cm, $\delta = 81.3°$, which is quite close to 90°. Thus, the small deviation of δ_{max} from 1.0 is not expected to be significant experimentally. Note that Ω decreases with increasing T.

(After this work was completed, we became aware of a paper by Kuznetsov and Ulstrup [21]. In the context of a different approach to the calculation of electron-transfer rates, they also speculate on the possibility of using electric field effects to test the hypothesis that photosynthetic electron transfer is activationless.)

VI. Summary

We have developed a method for the inclusion of coulombic and external field effects in calculations on photosynthetic electron transfer. Using this approach, we have been able to draw a number of conclusions.

(1) Reaction center geometry regulates photosynthetic electron-transfer dynamics not only through the tunneling matrix element, but also through the Franck-Condon factor ($\bar{\nu}_{\pm}$). This is accomplished through the effect of coulombic interaction of the electron being transferred with the hole it leaves behind – an interaction whose magnitude is crucially dependent on reaction center geometry*. Thus, bacterial photosynthesis provides another example of a biological energy-transduction system whose efficiency of operation is governed by correct placement of a neighboring charge.

(2) An estimate can be made of the electron intersite energy difference under operative conditions, for the transfer from bacteriopheophytin to the primary uniquinone. Under a particular set of assumptions as to parameter values and reaction center geometry, this is found to be 0.57 eV. The relation between this value and reaction center geometry and dielectric constant is exhibited.

(3) Use is made of experimental results on the reduction of the bacteriopheophytin → ubiquinone electron-transfer rate in the presence of reduced secondary quinone to place limits on the location of the secondary quinone in the reaction center.

(4) The temperature dependence of the electron-transfer rate in the presence of reduced secondary quinone is predicted.

(5) It is shown that the rate of electron transfer in the presence of an externally applied electric field is a function of reaction center orientation in the field, and that this effect can be used to test the hypothesis that the electron transfer is an activationless process.

As better values of the model parameters are determined, the method we have presented can be used to refine estimates of reaction center geometry and energetics.

These refined estimates are also subject the limitations inherent in our treatment of charge transfer. We can list some of the complications present in vivo which we have avoided. We have assumed only a monopole coulombic contribution to Δ from the charge distribution on $(BChl)_2$. The complexities of the orientational aspects of the intermolecular transfer have been incorporated into a parameterized, exponential tunneling element. The polarization of each molecule in response to its ionization has been described by a single molecular mode. The polarization response of the reaction center medium, on the time scale of the primary electron-transfer events, has been parameterized by a dielectric constant ϵ. The value of ϵ is not known. Values of $\epsilon = 2$–3 are typical in biological systems [19], however, $\epsilon = 6$ has been derived [24] from membrane capacitance measurements. We have chosen $\epsilon = 3$ and 4, but the calculations discussed in this paper can easily be extended to different values of ϵ. Our primary rationale for our simplifications is the focus on the large and measurable effects which have been listed at the beginning of this section.

Acknowledgements

We thank Professors R. Knox and P.L. Dutton for enlightening discussions and a critical reading of the manuscript.

References

1 Netzel, T.L., Leigh, J.S. and Rentzepis, P.M. (1973) Science 182, 238–241
2 Kaufman, K.J., Dutton, P.L., Netzel, T.L., Leigh, J.S. and Rentzepis, P.M. (1975) Science 188, 1301–1304
3 Kaufman, K.J., Petty, K.M., Dutton, P.L. and Rentzepis, P.M. (1976) Biochem. Biophys. Res. Commun. 70, 839–845
4 Leigh, J.S., Netzel, T.L., Dutton, P.L. and Rentzepis, P.M. (1974) FEBS Lett. 48, 136–140

* It is interesting to note that experimental evidence for 'distance-dependent Franck-Condon factors', which may be due to electrostatic interactions, has been adduced [22].

5 Netzel, T.L., Rentzepis, P.M., Tiede, D.M., Prince, R.C. and Dutton, P.L. (1977) Biochim. Biophys. Acta 460, 467–479
6 Rockley, M.G., Windsor, M.W., Cognell, R.J. and Parson, W.W. (1975) Proc. Natl. Acad. Sci. U.S.A. 72, 2251–2255
7 Peters, K., Avouris, P. and Renzepis, P.M. (1978) Biophys. J. 23, 207–217
8 Parson, W.W., Schenck, C.C., Blankenship, R.E., Holten, D., Windsor, M.W. and Schank, C.V. (1978) in Frontiers of Biological Energetics (Dutton, P.L., Leigh, J.S. and Scarpa, A., eds.), Academic Press, New York
9 Dutton, P.L., Leigh, J.L., Prince, R.C. and Tiede, D.M. (1979) in Light-Induced Charge Separation in Biology and Chemistry (Gerischer, H. and Katz, J.J., eds.), pp. 411–448, Verlag Chemie, Berlin.
10 Jortner, J. (1980) J. Am. Chem. Soc. 102, 6676–6686
11 Redi, M. and Hopfield, J.J. (1980) J. Chem. Phys. 72, 6651–6660
12 Packham, N.K., Packham, C., Mueller, P., Tiede, D.M. and Dutton, P.L. (1980) FEBS Lett. 110, 101–106
13 Pellin, M.J., Wright, C.A. and Kaufman, K.J. (1978) Biophys. J. 24, 361–369
14 Holstein, T. (1978) Philos. Mag. B. 37, 49–62
15 Holstein, T. (1978) Philos. Mag. B. 37, 499–526
16 Scher, H. and Holstein, T. (1981) Philos. Mag, B 44, 343–356
17 Nakanishi, K., Balogh-Nair, V., Tsujimoto, K. and Honig, B. (1980) J. Am. Chem. Soc. 102, 7945–7947
18 Honig, B., Dinur, U., Nakanishi, K., Balogh-Nair, V., Gawinowicz, M.A., Arnaboldi, M. and Motto, M.G. (1979) J. Am. Chem. Soc. 101, 7084–7086
19 Momany, F.A. McGuire, R.F., Burgess, A.W. and Scheraga, H.A. (1975) J. Phys. Chem. 79, 2361–2381
20 Witt, H.T. (1977) in Electrical Phenomena at the Biological Membrane Level (Roux, E., ed.), pp. 507–519, Elsevier,, New York
21 Kuznetsov, A.M. and Ulstrup, J. (1981) Biochim. Biophys. Acta 636, 50–57
22 Van Leeuwen, J.W., Heijman, M.G.J., Nauta, H. and Casteleijn, G. (1980) J. Chem. Phys. 73, 1483–1489
23 Tiede, D.M., Leigh, J.S. and Dutton, P.L. (1978) Biochim. Biophys. Acta 503, 524–544
24 Packham, N.J., Berriman, J.A. and Jackson, J.B. (1978) FEBS Lett. 89, 205–210